20th Australasian Fluid Mechanics Conference
Perth, Australia
5-8 December 2016

Transient Natural Convection Flow in a Cavity Subject to Time-Varying Sidewall Heating and Cooling

L. Zhou[1], S. W. Armfield[1], N. Williamson[1], M. P. Kirkpatrick[1] and Wenxian Lin[2]

[1]School of Aerospace, Mechanical and Mechatronic Engineering
The University of Sydney, Sydney, New South Wales 2006, Australia

[2]College of science and Engineering, Division of Tropical Environments and Societies
James Cook University, Townsville, Queensland 4811, Australia

Abstract

The flow development and behaviour of a fluid in a two-dimensional cavity, heated and cooled periodically from one sidewall, with all other walls adiabatic, is investigated via numerical simulation. The heating and cooling on the sidewall produce alternating direction vertical natural convection boundary layers that entrain fluid from the cavity interior and discharge it at the top and bottom of the cavity. At start up and during a transition phase the heat content of the cavity, which is biased by the initial heating phase, has a non-zero mean. At full development the flow is quasi steady with the natural convection boundary layers maintaining a stable stratification in the cavity interior and the heat content oscillating around a zero mean value. The stratification strength is shown to be strongly dependent on the forcing frequency.

Introduction

Natural convection flows occur in a variety of industrial and environmental settings, such as heating, ventilation and cooling in buildings, passive heat exchangers such as emergency cooling systems in nuclear reactors, crystallisation processes and magma chambers. A canonical model for many of these processes is the natural convection flow in a differentially heated cavity, typically with heating and cooling on opposing sidewalls and the remaining walls adiabatic. In most investigations the heated/cooled walls are maintained at constant temperatures, or constant heat flux [1, 2, 3, 8, 9], whereas in many applications the heating/cooling is time varying, such as in the diurnal solar heating of buildings .

In this investigation the two-dimensional natural convection flow of a fluid at Prandtl number 7.0 in a square cavity is considered. A sinusoidal temperature boundary condition, with zero mean, is applied on the left hand sidewall, with the remaining walls adiabatic and all walls non-slip. Previous investigations have considered periodic forcing of differentially side-heated cavities, with non-zero mean, with the aim of generating resonance to increase the heat transfer, as well as examining the basic flow structure [4, 5, 6, 7, 10].

The flow considered here is initially quiescent and at zero non-dimensional temperature. The periodic heating and cooling of the forcing produces alternating direction natural convection boundary layers that entrain fluid from the cavity interior and discharge it as hot and cold intrusions at the top and bottom of the cavity, respectively. The alternative discharge of hot and cold fluid into the cavity leads to a periodic variation in the heat content of the cavity, with an initial positive mean bias as a result of the initial heating phase of the periodic boundary condition. After an initial development time the flow becomes quasi steady, with the heat content varying periodically about a zero mean value. At full development the alternating direction natural convection boundary layers act to maintain a quasi-steady stable stratification in the cavity interior.

Numerical Method

The governing equations are the Navier-Stokes equations, in two-dimensional incompressible form with the Oberbeck-Boussinesq approximation for buoyancy, together with the temperature transport equation,

$$U_t + UU_x + VU_y = -P_x + \frac{\Pr}{\mathrm{Ra}^{\frac{1}{2}}}(U_{xx} + U_{yy}), \quad (1)$$

$$V_t + UV_x + VV_y = -P_y + \frac{\Pr}{\mathrm{Ra}^{\frac{1}{2}}}(V_{xx} + V_{yy}) + \Pr T, \quad (2)$$

$$U_x + V_y = 0, \quad (3)$$

$$T_t + UT_x + VT_y = \frac{1}{\mathrm{Ra}^{\frac{1}{2}}}(T_{xx} + T_{yy}). \quad (4)$$

Here U and V are velocities in the x and y directions, respectively, and P and T are pressure and temperature. The subscripts represent partial differentiation with respect to the x and y directions and to time t. The equations are written in non-dimensional form in terms of the characteristic length scale H, the height and width of the square cavity, the temperature difference ΔT, which is half of the difference between the maximum and minimum forcing temperature, and the characteristic velocity defined as $\mathbf{U} = (g\beta\Delta T H)^{1/2}/\Pr^{1/2}$ where β is the coefficient of thermal expansion for the fluid and κ and ν are the thermal diffusivity and kinematic viscosity of the fluid, respectively. The Rayleigh number is defined as $\mathrm{Ra} = (g\beta\Delta T H^3)/(\nu\kappa)$ and the Prandtl number is $\Pr = \nu/\kappa$.

All spatial derivatives in the Navier-Stokes equations and in the temperature transport equation are discretised using a two-step compact fourth-order approach [11]. The equations are integrated in time using an Adams-Bashforth approach for the advection terms and a deferred correction Crank-Nicolson approach for the viscous/diffusion terms. The resultant linear system is solved at each time step using the Jacobi method with a residual criterion of 1×10^{-4}. The pressure is updated and continuity is enforced using a pressure-correction approach, where the pressure derivatives are discretised with second-order differences and the approximate divergence is discretised using a compact fourth-order scheme. The resulting linear system is solved for the pressure correction using a Gauss-Seidel method with a residual criterion of 1×10^{-4}. The pressure correction is then used to project the velocities onto a divergence free velocity field, and to update the pressure, completing the time-step. This scheme has been shown to provide overall fourth-order spatial accuracy [11].

The computational domain is a square cavity $\Omega \in [0,1] \times [0,1]$.

The initial and boundary conditions are,

$$U = V = T = 0 \quad \text{in } \Omega \text{ when } t = 0, \tag{5}$$

$$U = V = 0 \quad \text{on } x = 0,\ 1;\ y = 0,\ 1, \tag{6}$$

$$T_x = 0 \quad \text{on } x = 1, \tag{7}$$

$$T_y = 0 \quad \text{on } y = 0,\ 1, \tag{8}$$

$$T = \sin(2f\pi t) \quad \text{on } x = 0, \tag{9}$$

with f the frequency of the time varying boundary condition.

Results have been obtained for Rayleigh numbers $\text{Ra} = 1 \times 10^6$ and $\text{Ra} = 1 \times 10^8$. For the lower Ra a 100×100 nonuniform rectangular grid is used, with the finest cells adjacent to the sidewalls, and the top/bottom, where $\Delta x \cong 0.005$ and $\Delta y \cong 0.005$, respectively. The grid is then stretched towards the centre, with an expansion ratio of 1.03, giving a largest cell in the centre of the cavity of approximately 0.02×0.02. The equations are integrated from $t = 0$ to full development at $t \cong 1000$ with the time step $\Delta t = 2 \times 10^{-3}$. For the higher Ra a 200×200 nonuniform rectangular grid is used with half the grid-size and time-step of that for the lower Ra.

Results

Results are presented for the start up and development of the flow at $\text{Ra} = 1 \times 10^6$ and 1×10^8 at $\text{Pr} = 7.0$. The basic flow structure is shown in figure 1 where the stream function and temperature contours for $\text{Ra} = 1 \times 10^6$, with a forcing frequency $f = 0.2$, are presented. The first three times shown, $t = 2.5, 5$ and 7.5 correspond to the ends of the initial heating phase, the initial cooling phase, and the second heating phase, at this frequency. The final time, $t = 1000$, shows the fully developed structure during a cooling phase.

At the conclusion of the initial heating phase, $t = 2.5$, a natural convection boundary layer has formed travelling up the left, heated, wall, discharging into a buoyant, hot, intrusion at its downstream end, the top left corner of the domain. The intrusion and natural convection boundary layer are clearly visible in figure 1a, with the intrusion extending approximately one third of the way across the domain beneath the adiabatic upper boundary. The initial natural convection boundary layer and intrusion are seen, in the stream function contours, to be associated with a clockwise circulation spanning the full cavity. The natural convection boundary layer entrains fluid from the cavity interior over, approximately, the lower 80% of its extent.

The sidewall forcing is in the first cooling phase of the cycle from $t = 2.5$ to $t = 5$. The results at $t = 5$, the end of the first cooling phase, in figure 1b, show a negatively buoyant natural convection boundary layer adjacent to the cooled wall, discharging into a negatively buoyant, cool, intrusion at its downstream end, the lower left corner of the domain. The cooled intrusion extends approximately one third of the way across the domain, immediately above the bottom adiabatic boundary. The remainder of the buoyant, hot, intrusion, from the previous heating phase, can be seen immediately below the upper boundary, now spanning approximately 80% of the domain width, but with reduced intensity when compared to its structure in figure 1a. The negatively buoyant natural convection boundary layer and cool intrusion are seen to be associated with a counter-clockwise circulation. At this stage the natural convection boundary layer entrains fluid from the cavity interior over, approximately, the upper 80% of its extent. The natural convection boundary layer circulation does not span the full domain, with a region of clockwise circulation seen in the upper right corner of the domain, a residual of the cavity scale circulation generated in the first heating phase, described above.

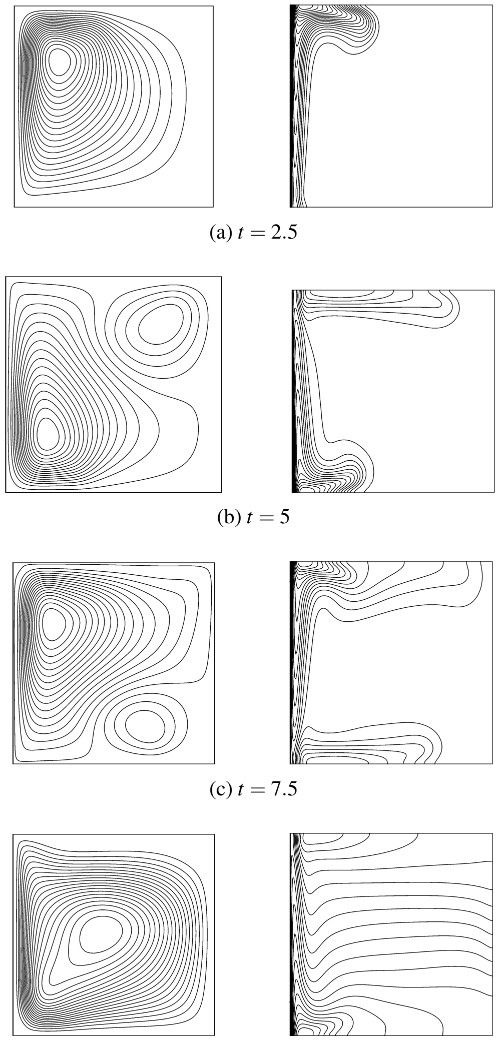

(a) $t = 2.5$

(b) $t = 5$

(c) $t = 7.5$

(d) $t = 1000$

Figure 1: Contours of the stream function (left) and temperature (right) for $f = 0.2$ and $\text{Ra} = 1 \times 10^6$ at $t = 2.5$, $t = 5$, $t = 7.5$ and $t = 1000$.

The results in figure 1c, at the conclusion of the second heating phase at $t = 7.5$, show a natural convection boundary layer travelling up the now heated left-hand wall, discharging into a heated intrusion that has merged with the residual of the heated intrusion from the first heating phase. The resultant hot, buoyant, fluid now spans the full cavity width immediately beneath the upper boundary. The stream function contours show an associated clockwise circulation over the height of the cavity, with a residual counter-clockwise circulation, from the cooling phase, in the lower right corner.

The further development of the flow follows the basic pattern observed for the initial heating/cooling/heating phases described above. Alternating rising and falling natural convection boundary layers form adjacent to the left hand wall, discharging heated/cooled fluid into the cavity interior below/above the top/bottom boundaries. The rising/falling boundary layers entrain some, but not all, of the fluid discharged by the previous falling/rising boundary layers, leading to a gradual increase in the heated/cooled fluid in upper/lower part of the cavity interior. Ultimately this leads to the discharged fluid filling the cavity and a stratified cavity interior. Figure 1d shows the fully developed flow during a cooling phase, with a falling natural convection boundary layer adjacent to the cooled left hand wall, and

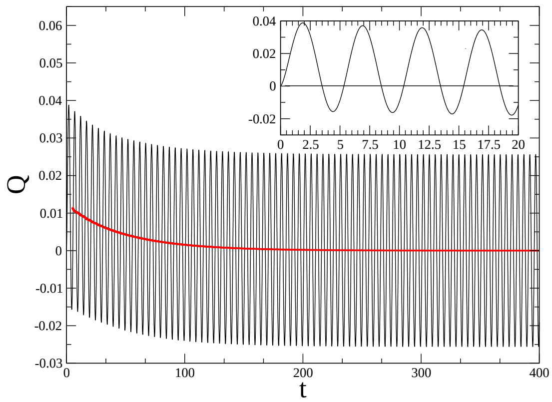

Figure 2: Total heat content Q for $f = 0.2$ and $\mathrm{Ra} = 1 \times 10^6$.

a counter clockwise circulation spanning the full cavity. The fully developed flow then consists of alternating direction natural convection boundary layers adjacent to the left hand wall, with associated alternating direction cavity scale circulations. The natural convection boundary layers entrain fluid from, and discharge fluid to, the cavity interior, perturbing the stable temperature stratification. Thus one of the main outcomes of the alternating heating and cooling is the generation and maintenance of a quasi-steady approximately linear stable stratification in the interior of the cavity.

A measure of the effect of the alternating heating and cooling is the total heat content of the cavity fluid, Q, obtained by integrating the temperature over the domain. The heat content time series over eighty heating/cooling cycles, $t = 0$ to 400, is presented in figure 2, showing the start up and transition to fully developed quasi-steady flow. The bold red line is a running average of Q, and the heat content oscillates about its average value with the same frequency as the forcing. The heat content is initially positive biased, with the bias reducing with time, approaching zero at full development when the flow is quasi steady. The inset shows Q from $t = 0$ to 20, the initial four heating/cooling cycles allowing the initial biasing to be viewed in more detail. During the first heating phase the heat content peaks at $Q \sim 0.04$ at $t \sim 2$. The sidewall temperature peaks at $t = 1.25$, and thus the heat content peaks after the sidewall temperature peaks. The first minimum in Q is ~ 0.15, 37% of the first maximum, at $t \sim 4.5$, whereas the first minimum in the sidewall temperature occurs at $t = 3.75$. In subsequent heating/cooling phases the respective maxima and minima of Q gradually reduce until, at full development, they are symmetric about zero, as observed in the longer time series. The phase offset of approximately $\delta t = 0.75$ remains constant through the full development of the flow.

As noted above one of the major effects of the oscillating boundary condition is to establish an approximately linear quasi-steady stable stratification in the cavity at full development. The stratification can be quantified by the stratification parameter,

$$S = \int_{\Omega} T_y \, d\omega. \qquad (10)$$

Time series of S for a range of f are plotted in figures 3 and 4 for Rayleigh numbers $\mathrm{Ra} = 1 \times 10^6$ and $\mathrm{Ra} = 1 \times 10^8$, respectively. Again, as for Q above, S is seen to have an initial development stage, transiting ultimately to a quasi-steady structure, oscillating around a constant mean value. Considering the $\mathrm{Ra} = 1 \times 10^6$ case, it is seen that the average value of S at full development varies considerably from a minimum of approximately 0.15 at $f = 2$ to a maximum of approximately 0.79 at $f = 0.02$. The variation in the average S is seen to be non-monotonic, increasing with frequency from $f = 0.002$ to the maximum at $f = 0.02$, then decreasing with further increase in frequency.

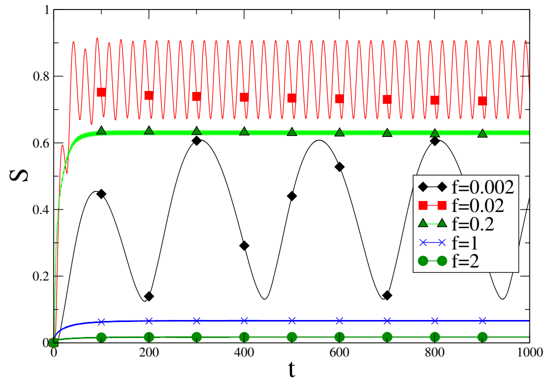

Figure 3: Stratification parameter S for $\mathrm{Ra} = 1 \times 10^6$

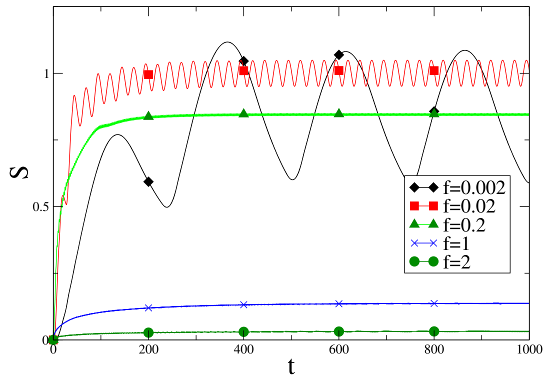

Figure 4: Stratification parameter S for $\mathrm{Ra} = 1 \times 10^8$

The time series for the $\mathrm{Ra} = 1 \times 10^8$ case, in figure 4, show the same general behaviour as for the lower Ra case, with minor Ra dependent effects. The stratification parameter S is again seen to transit through an initial development phase to a quasi-steady fully developed phase where it oscillates about a constant mean. For the frequencies considered the maximum average value of S at full development is approximately 1 at $f = 0.02$, and the minimum approximately 0.03 at $f = 2$. The average value of S at full development for the $f = 0.002$ is again less than that at $f = 0.02$, although the variation is smaller than it was for the lower Rayleigh number case.

The stratification is maintained by the balance between the entrainment of stratified fluid from the cavity interior by the natural convection boundary layers and the discharge of heated/cooled fluid at the down stream corners of the boundary layers during each heating/cooling phase. At higher frequencies the volume of fluid discharged during each heating/cooling phase is reduced due to the reduced time available, and for $f \gtrsim 1$ the natural convection boundary layer itself will not reach full development during each heating/cooling phase. The reduced discharge at higher f leads to a reduction in the intensity of the stratification. At low enough frequencies the forcing period is comparable to the time for the natural convection boundary layer to completely fill the cavity. Once the cavity is fully stratified it will, in the heating phase for example if the period is such that it exceeds the time to fully stratify the cavity, then continue to fill the cavity from the top down with unstratified fluid at, or near to, the temperature of the heated boundary, increasing the temperature of the fluid adjacent to the bottom boundary. This means that at low enough frequency the stratification will be reduced, as observed here.

Conclusion

Numerical simulations have been obtained for natural convection flow in a cavity with a time-varying, sinusoidal, temperature boundary condition on one sidewall, with all other walls adiabatic and all walls non-slip. The time-varying boundary condition produces alternating direction natural convection boundary layers adjacent to the sidewall. The natural convection boundary layers entrain fluid from the cavity interior over most of their upstream regions, discharging heated/cooled fluid into the cavity interior in the form of intrusions at their downstream corners. These processes of cyclic entrainment and discharge act to generate and maintain a stratification in the cavity interior.

During the start-up period the total heat content of the cavity is biased by the initial heating phase of the boundary condition, so that the average of the heat content over a single heating/cooling cycle is positive. As the flow progresses to a fully developed state the heat content becomes quasi-steady, oscillating about a zero average value.

A stratification parameter has been obtained by integrating the vertical derivative of temperature over the cavity domain. This parameter transits through a similar start-up period as that of the total heat content, ultimately transiting to a fully developed quasi-steady state. The stratification parameter is observed to have a maximum value at an intermediate forcing frequency of $f = 0.02$ for the range of frequencies considered here, at both $\mathrm{Ra} = 1 \times 10^6$ and $\mathrm{Ra} = 1 \times 10^8$. For smaller f the stratification reduces because the forcing period is then greater than the time required to fully stratify the cavity interior, and the continuing natural convection boundary layer discharge then acts to destratify the cavity interior. For larger f the reduced forcing period reduces the volume of the natural convection boundary layer discharge for each heating/cooling phase, reducing the ability of the discharges to maintain the stratification.

Acknowledgements

The authors acknowledge the support of the Australian Research Council.

References

[1] De Vahl Davis, G., Laminar natural convection in an enclosed rectangular cavity, *Int. J. Heat Mass Transfer*, **11**, 1968,1675-1693.

[2] De Vahl Davis, G., Natural convection of air in a square cavity: A bench mark numerical solution, *Int. J. Numer. Meth. Fluids*, **3**, 1983, 249-264.

[3] Hyun, J. M., in *Advances in Heat Transfer*, (ed. James P. Hartnett, T. F. I. and Y. I. C.) **24**, Elsevier 1994, 277-320.

[4] Kazmierczak, M. and Chinoda, Z., Buoyancy-driven flow in an enclosure with time periodic boundary conditions, *Int. J. Heat Mass Transfer* **35**, 1992, 1507-1518.

[5] Kwak, H. S. and Hyun, J. M., Natural convection in an enclosure having a vertical sidewall with time-varying temperature, *J. Fluid Mech.*, **329**, 1996, 65-88.

[6] Lage, J. L. and Bejan, A., The resonance of natural convection in an enclosure heated periodically from the side, *Int. J. Heat Mass Transfer*, **36**, 1993, 2027-2038.

[7] Lin, W. and Armfield, S. W., Long-term behavior of cooling fluid in a rectangular container, *Phys. Rev. E*, **69**, 2004, 56315.

[8] Patterson, J. C. and Armfield, S. W., Transient features of natural convection in a cavity, *J. Fluid Mech.*, **219**, 1990, 469-497.

[9] Patterson, J. and Imberger, J., Unsteady natural convection in a rectangular cavity, *J. Fluid Mech.*, **100**, 1980, 65-86.

[10] Reima, I., Hyun, J. M. and Kunio, K., Convection in a differentially-heated square cavity with a torsionally-oscillating lid, *Int. J. Heat Mass Transfer*, **35**, 1992, 1069-1076.

[11] Zhou, L. and Armfield, S. W., A compact fourth-order spatial discretisation applied to the Navier-Stokes equations, *ANZIAM J.*, **56**, 2016, C481-C501.